



## Benzothiophene piperazine and piperidine urea inhibitors of fatty acid amide hydrolase (FAAH)

Douglas S. Johnson<sup>a,b,\*</sup>, Kay Ahn<sup>a,b</sup>, Suzanne Kesten<sup>a</sup>, Scott E. Lazerwith<sup>a</sup>, Yuntao Song<sup>a</sup>, Mark Morris<sup>a</sup>, Lorraine Fay<sup>a</sup>, Tracy Gregory<sup>a,b</sup>, Cory Stiff<sup>a,b</sup>, James B. Dunbar Jr.<sup>a</sup>, Marya Liimatta<sup>a,c</sup>, David Beidler<sup>a,d</sup>, Sarah Smith<sup>a,d</sup>, Tyzoon K. Nomanbhoy<sup>e</sup>, Benjamin F. Cravatt<sup>f</sup>

<sup>a</sup> Pfizer Global Research and Development, 2800 Plymouth Road, Ann Arbor, MI 48105, USA

<sup>b</sup> Pfizer Global Research and Development, Eastern Point Road, Groton, CT 06340, USA

<sup>c</sup> Pfizer Global Research and Development, 620 Memorial Drive, Cambridge, MA 02139, USA

<sup>d</sup> Pfizer Global Research and Development, 700 Chesterfield Parkway, Chesterfield, MO 63017, USA

<sup>e</sup> ActivX Biosciences, 11025 North Torrey Pines Road, La Jolla, CA 92037, USA

<sup>f</sup> Department of Chemical Physiology, The Skaggs Institute for Chemical Biology, The Scripps Research Institute, 10550 North Torrey Pines Road, La Jolla, CA 92037, USA

### ARTICLE INFO

#### Article history:

Received 24 February 2009

Revised 16 March 2009

Accepted 20 March 2009

Available online 24 March 2009

#### Keywords:

FAAH inhibitor

Fatty acid amide hydrolase

Urea

Activity-based protein profiling

Covalent inhibitor

### ABSTRACT

The synthesis and structure–activity relationships (SAR) of a series of benzothiophene piperazine and piperidine urea FAAH inhibitors is described. These compounds inhibit FAAH by covalently modifying the enzyme's active site serine nucleophile. Activity-based protein profiling (ABPP) revealed that these urea inhibitors were completely selective for FAAH relative to other mammalian serine hydrolases. Several compounds showed *in vivo* activity in a rat complete Freund's adjuvant (CFA) model of inflammatory pain.

© 2009 Elsevier Ltd. All rights reserved.

Fatty acid amide hydrolase (FAAH) is an integral membrane enzyme that degrades the fatty acid amide family of signaling lipids, including the endocannabinoid anandamide.<sup>1</sup> Genetic<sup>1g</sup> or pharmacological<sup>1f</sup> inactivation of FAAH leads to elevated endogenous levels of fatty acid amides and a range of behavioral effects including analgesic and anti-inflammatory phenotypes in rodents. Importantly, these behavioral phenotypes occur in the absence of alterations in motility, weight gain, or body temperature that are typically observed with direct cannabinoid receptor 1 (CB1) agonists, indicating that FAAH may represent an attractive therapeutic target for the treatment of inflammatory pain and related conditions.<sup>2</sup> Several classes of FAAH inhibitors have been reported including electrophilic ketones (e.g., OL-135<sup>3</sup>), carbamates (e.g., URB597<sup>4</sup> and SA-47<sup>5</sup>) and, more recently, piperidine/piperazine ureas (e.g., PF-750<sup>6</sup> and Takeda-25/JNJ-1661010<sup>7</sup>) (Fig. 1). We recently reported that PF-750 inhibits FAAH by covalently modifying the enzyme's active site serine nucleophile and is completely selective for FAAH relative to other mammalian serine hydrolases.<sup>6a</sup> In this Letter, we describe the synthesis and struc-

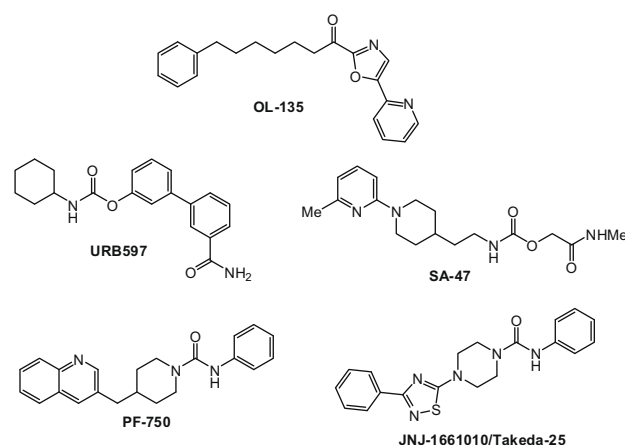


Figure 1. Structures of FAAH inhibitors.

ture–activity relationships (SAR) of a series of benzothiophene piperazine and piperidine urea FAAH inhibitors.

A series of piperazine phenyl ureas, exemplified by **1**, was discovered by high throughput screening of the Pfizer chemical file

\* Corresponding author.

E-mail address: [doug.johnson@pfizer.com](mailto:doug.johnson@pfizer.com) (D.S. Johnson).

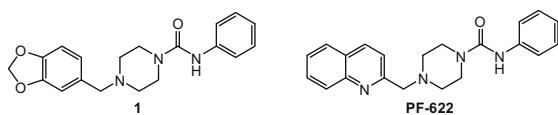


**Figure 2.** Structures of HTS lead (**1**) and PF-622.

against human FAAH (Fig. 2). We prepared piperazine phenyl urea intermediate **2** and performed a series of reductive aminations with various aromatic aldehydes (Scheme 1, Eqs. 1 and 2). This allowed us to easily vary the aldehyde component and resulted in the identification of several bicyclic cores including PF-622<sup>6a</sup> and a series of benzothiophenes represented by **4h** which is the subject of this manuscript (Scheme 1, Eq. 2).

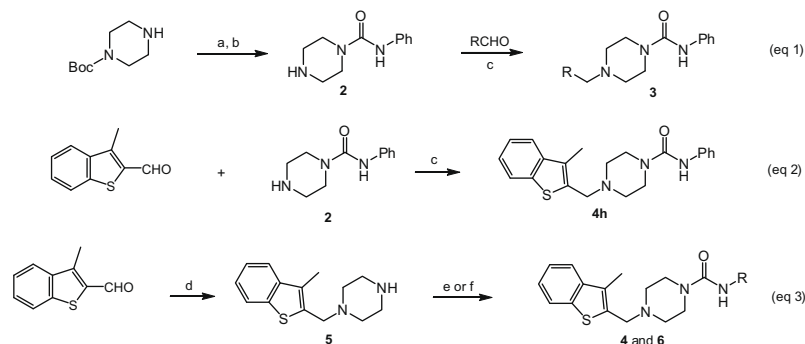
We then explored the benzothiophene lead **4h** in more detail. Therefore, the benzothiophene piperazine intermediate **5** was prepared according to equation 3 and reacted with various commercially available alkyl and aryl isocyanates or phenyl carbamates of heterocyclic amines<sup>8</sup> to give the corresponding piperazine ureas **4** and **6** (Scheme 1).

Schemes 2 and 3 outline the synthesis of representative piperidine urea FAAH inhibitors utilized in the current studies. Lithiation of benzothiophene **7** followed by reaction with Weinreb amide **8** provided ketone **9** in good yield.<sup>9</sup> Ketone **9** was reduced with sodium borohydride to give alcohol **10** which underwent elimination when treated with *p*-toluene sulfonic acid (TsOH). The resulting double bond was hydrogenated to give piperidine **11** which was treated with isocyanate **12** as described previously to give the desired urea **13**.<sup>8</sup>

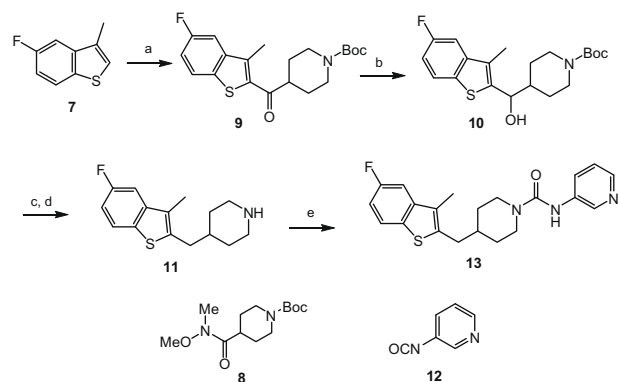
The linker analogs **15–18** were synthesized according to Scheme 3. Deprotection of Boc-piperidine **14** with TFA followed by reaction with isocyanate **12** afforded urea **15** with a ketone linker. Wittig olefination of ketone **15** provided compound **16** with a methylene substituted linker. Hydrogenation of the double bond gave **17** with a methyl substituted linker as the racemate and the enantiomers were separated by chiral chromatography. Furthermore, ketone **15** was reduced to give racemic **18** with a hydroxy substituted linker.

As previously reported, these piperidine/piperazine ureas inhibit FAAH by covalent carbamylation of the catalytic Ser241 nucleophile.<sup>6a,b</sup> Therefore, the potency of these benzothiophene piperidine/piperazine urea inhibitors were determined by the second order rate constants  $k_{\text{inact}}/K_i$  values using an enzyme-coupled FAAH assay as described previously.<sup>6b,10</sup> Unlike  $IC_{50}$  values,  $k_{\text{inact}}/K_i$  values do not change with various preincubation times and have been described as the best measure of potency for irreversible inhibitors.<sup>11</sup>

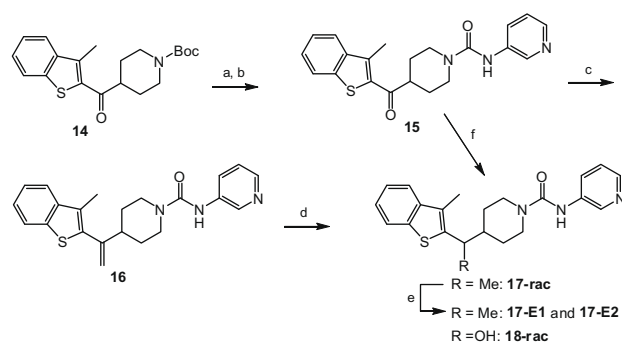
Table 1 shows the SAR of the right hand portion of the urea. The alkyl ureas (**4a–g**) had very low potency for FAAH, which is similar



**Scheme 1.** Synthesis of piperazine ureas **4** and **6**: (a) PhNCO, CH<sub>2</sub>Cl<sub>2</sub>, 92%; (b) TFA, CH<sub>2</sub>Cl<sub>2</sub>, 80–99% (c) NaBH(OAc)<sub>3</sub>, DCE, 50–95%; (d) *N*-Boc-piperazine, NaBH(OAc)<sub>3</sub>, CH<sub>2</sub>Cl<sub>2</sub>; then TFA, CH<sub>2</sub>Cl<sub>2</sub>, 64%; (e) RNCO (R = alkyl, Ph, 3-pyr; ie. **4d–g**, **4h**, **6a**), CH<sub>2</sub>Cl<sub>2</sub>, 50–90%; (f) RNHCO<sub>2</sub>Ph (R = heterocycle, ie. **4j–1**, **6**), DMSO, 60 °C, 50–80%.



**Scheme 2.** Synthesis of piperidine urea **13**: (a) *n*-BuLi, THF, –78 °C; then add **8**, 70%; (b) NaBH<sub>4</sub>, EtOH, quant; (c) TsOH, toluene, quant; (d) H<sub>2</sub>(g), 20% Pd/C, MeOH, 87%; (e) **12**, CH<sub>2</sub>Cl<sub>2</sub>, 60%.

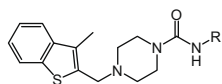


**Scheme 3.** Synthesis of linker analogs **15–18**: (a) TFA, CH<sub>2</sub>Cl<sub>2</sub>, 99%; (b) **12**, CH<sub>2</sub>Cl<sub>2</sub>, 85%; (c) Ph<sub>3</sub>PCH<sub>3</sub>Br, *n*-BuLi, THF, –20 °C to rt, 97%; (d) H<sub>2</sub>(g), Pd/C, MeOH, 76%; (e) chiral chromatography (CHIRALCEL® OD); (f) NaBH<sub>4</sub>, EtOH, quant.

to what has been observed for *N*-alkyl urea analogs of URB597.<sup>4a</sup> In contrast, we found that aryl ureas such as phenyl urea **4h** were potent FAAH inhibitors. Next, we investigated a series of heteroaromatic ureas (**4i–l**, **6a**) in part to avoid the generation of aniline upon covalent binding to FAAH. The 3-aminopyridyl group (**6a**) was preferred over the 2-aminopyridyl (**4i**) and 3-aminopyridazinyl (**4j**) groups in the benzothiophene series. The SAR of the heterocyclic group was highly sensitive. For example, isoxazole **4k** retained potency, while the potency was lost with methylthiazole **4l**, which is consistent with observations made by Keith et al. in a related thiadiazolopiperazinyl urea series.<sup>7b</sup> Boger and co-workers also observed that subtle changes in the central heterocycle of  $\alpha$ -ketoheterocycle FAAH inhibitors greatly influence inhibitor activ-

**Table 1**

Human and rat FAAH potency ( $k_{\text{inact}}/K_i$  values)<sup>15</sup> for compounds **4a–I**, **6a** showing SAR of the right hand side of the urea



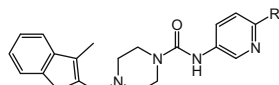
R	$h k_{\text{inact}}/K_i$ ( $\text{M}^{-1} \text{s}^{-1}$ )	$r k_{\text{inact}}/K_i$ ( $\text{M}^{-1} \text{s}^{-1}$ )	
<b>4a</b>	Butyl	44	13
<b>4b</b>	CH <sub>2</sub> CH <sub>2</sub> OH	42	<10
<b>4c</b>	CH <sub>2</sub> C(O)NHMe	<10	<10
<b>4d</b>	<i>i</i> Pr	70	<10
<b>4e</b>	Cyclohexyl	<10	<10
<b>4f</b>	<i>t</i> Bu	<10	<10
<b>4g</b>	Bn	<10	<10
<b>4h</b>	Ph	1918	762
<b>4i</b>	2-pyr	1002	635
<b>6a</b>	3-pyr	2401	1083
<b>4j</b>		924	191
<b>4k</b>		1559	1433
<b>4l</b>		<10	<10

ity.<sup>3c</sup> Also it is interesting to note that isoxazole **4k** exhibited equal potency for hFAAH and rFAAH, while phenyl urea **4h** and pyridazine urea **4j** showed higher potency for hFAAH than rFAAH.

Next, we investigated the effect of substituents at the 6-position of the 3-amino pyridine (Table 2). The compounds with 6-methoxy (**6g**), 6-amino (**6i**) and 6-NHAc (**6n**) substituents are roughly equipotent to **6a**, while the 6-Cl (**6d**) and 6-NHMe (**6j**) groups result in compounds that are about twofold less potent and the potency is further diminished by the 6-NHEt (**6l**) substituent (fourfold less potent than **6a**). Furthermore, 6- $\text{CF}_3$  (**6c**) and 6- $\text{NEt}_2$  (**6m**) substituents are detrimental to activity. Taken together with the results in Table 1, it is clear that the nature of the aromatic amine portion of the urea is critical for activity, but the potency does not appear to correlate with the leaving group ability. There appears to be a steric limitation at the 6-position as hFAAH potency generally decreases with the larger substituents (i.e.,  $h k_{\text{inact}}/K_i$  for  $\text{NH}_2 > \text{NHMe} > \text{NMe}_2 > \text{NEt}_2$ ). Interestingly, several 6-amino compounds (**6j–m**) actually show a preference for rFAAH over hFAAH.

**Table 2**

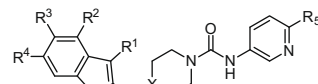
Human and rat FAAH potency ( $k_{\text{inact}}/K_i$  values)<sup>15</sup> for compounds **6a–6n** showing SAR of substituted pyridyl ureas



R	$h k_{\text{inact}}/K_i$ ( $\text{M}^{-1} \text{s}^{-1}$ )	$r k_{\text{inact}}/K_i$ ( $\text{M}^{-1} \text{s}^{-1}$ )	
<b>6a</b>	H	2401	1083
<b>6b</b>	Me	1481	390
<b>6c</b>	$\text{CF}_3$	69	<10
<b>6d</b>	Cl	1238	242
<b>6e</b>	Br	645	157
<b>6f</b>	Ph	631	1215
<b>6g</b>	OMe	2931	1060
<b>6h</b>	O-(3-Pyr)	605	101
<b>6i</b>	$\text{NH}_2$	1871	1067
<b>6j</b>	NHMe	1108	1513
<b>6k</b>	$\text{NMe}_2$	892	1811
<b>6l</b>	NHEt	597	1891
<b>6m</b>	$\text{NEt}_2$	90	227
<b>6n</b>	NHAc	2011	1719

**Table 3**

Human and rat FAAH potency ( $k_{\text{inact}}/K_i$  values)<sup>15</sup> for compounds **13**, **19–39** showing SAR of substituted benzothiophenes



R <sup>1</sup>	R <sup>2</sup>	R <sup>3</sup>	R <sup>4</sup>	R <sup>5</sup>	X	$h k_{\text{inact}}/K_i$ ( $\text{M}^{-1} \text{s}^{-1}$ )	$r k_{\text{inact}}/K_i$ ( $\text{M}^{-1} \text{s}^{-1}$ )	
<b>19</b>	H	H	H	H	N	695	174	
<b>6a</b>	Me	H	H	H	N	2401	1083	
<b>20</b>	Me	H	H	H	C	5129	2613	
<b>21</b>	Et	H	H	H	N	1402	774	
<b>22</b>	Et	H	H	H	C	1668	1013	
<b>6b</b>	Me	H	H	Me	N	1481	390	
<b>23</b>	Cl	H	H	Me	N	900	133	
<b>24</b>	Me	F	H	H	N	3321	1203	
<b>25</b>	Me	F	H	H	C	4147	1547	
<b>26</b>	Me	F	H	H	N	1980	758	
<b>27</b>	Me	H	F	H	N	3134	779	
<b>13</b>	Me	H	F	H	C	4474	729	
<b>28</b>	Me	H	Me	H	N	2635	557	
<b>29</b>	Me	H	Me	H	C	3024	482	
<b>30</b>	Me	H	Cl	H	N	2822	1133	
<b>31</b>	Me	H	$\text{CF}_3$	H	N	1389	219	
<b>32</b>	Me	H	OMe	H	N	1381	500	
<b>33</b>	Et	H	F	H	N	1808	617	
<b>34</b>	Et	H	F	H	C	2292	1141	
<b>35</b>	Me	H	F	Me	N	1871	260	
<b>36</b>	Me	H	Me	H	N	1169	183	
<b>37</b>	Me	H	H	OMe	H	N	73	113
<b>38</b>	Me	H	H	OEt	H	N	14	<10
<b>39</b>	Cl	H	H	Me	Me	N	73	14

Subsequent SAR studies focused on optimization of the benzothiophene substitution while maintaining the optimal 3-aminopyridyl urea (Table 3). It was found that incorporating an alkyl group at the 3-position of the benzothiophene ( $R^1$ ) led to improved potency. For example, compound **6a** was 3–4-fold more potent than the unsubstituted benzothiophene **19**. In most cases for hFAAH, the piperidine analogs were slightly more potent than the corresponding piperazine analogs (i.e., **20** > **6a**), which is most likely a result of more favorable Van der Waals interactions of the piperidine with the acyl chain binding channel of FAAH.<sup>1b,6b</sup> Substitution was tolerated at the 4- and 5-position of the benzothiophene (**24–36**), but no significant improvement in potency was realized. Conversely, moving the substituent ( $R^4$ ) to the 6-position of the benzothiophene impaired potency (**37–39**), which is predicted to introduce steric clashes with the FAAH protein (Fig. 5).

As shown in Table 4, the potency is maintained when a ketone or methylene is incorporated within the linker (**15** and **16**, Scheme 3) whereas the reduced compounds **17** and **18** with methyl and hydroxyl substituents lose much of their activity. The  $\text{sp}^2$  hybridization of the ketone and methylene linker compounds **15** and **16** imposes a conformational constraint that appears to help position the benzothiophene in a more favorable binding orientation. The SAR in this linker region is sensitive as further evidenced by the >10-fold difference in potency for the enantiomers of **17**.

**Table 4**

Human and rat FAAH potency ( $k_{\text{inact}}/K_i$  values)<sup>15</sup> for compounds **15–18** showing SAR of the piperidine linker

	$h k_{\text{inact}}/K_i$ ( $\text{M}^{-1} \text{s}^{-1}$ )	$r k_{\text{inact}}/K_i$ ( $\text{M}^{-1} \text{s}^{-1}$ )
<b>15</b>	3601	1226
<b>16</b>	5441	991
<b>17-rac</b>	114	48
<b>17-E1</b>	34	<10
<b>17-E2</b>	617	110
<b>18-rac</b>	200	79

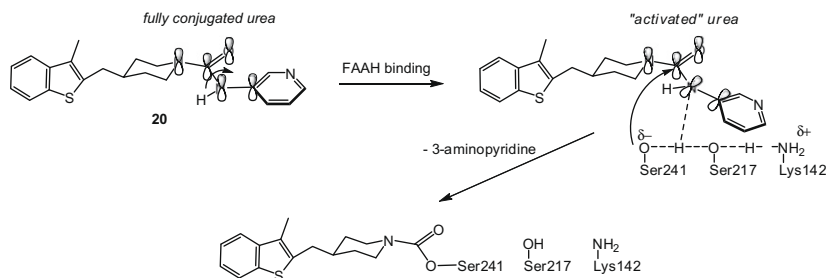


**Figure 3.** Proposed mechanism of covalent inhibition of FAAH by piperidine ureas. The catalytic triad Ser-Ser-Lys is shown.

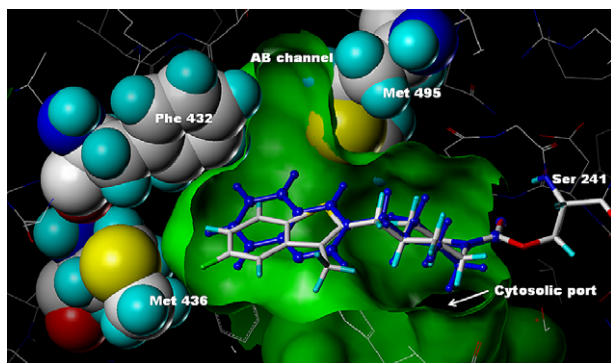


**Figure 4.** Model of compound **13** covalently attached to Ser241 of h/rFAAH using coordinates from the PF-750-h/rFAAH crystal structure.<sup>6b</sup> Overlay with PF-750 shown in blue.

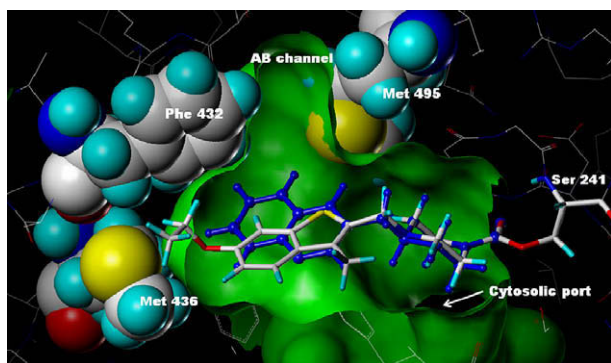


**Figure 5.** Model of compound **38** covalently attached to Ser241 of h/rFAAH using coordinates from the PF-750-h/rFAAH crystal structure.<sup>6b</sup> Overlay with PF-750 shown in blue.

We have proposed that the urea may be activated upon binding in the active site of FAAH by undergoing a conformational change that diminishes conjugation of the nitrogen lone pair with the carbonyl, which would activate the urea toward nucleophile attack as shown in Figure 3.<sup>6a</sup> It appears that a cyclic secondary amine such as piperazine or piperidine is critical for activation of the urea as ureas prepared from primary amines are ineffective.<sup>4a</sup>

Compound **13** (Fig. 4) and compound **38** (Fig. 5) were modeled,<sup>12</sup> using Sybyl 8.0, into the ‘humanized’ rat FAAH (h/rFAAH) crystal structure (2VYA).<sup>6b</sup> Compound **13** fit within the binding site in almost identical fashion to that of PF-750 with only very slight movement of the surrounding residue atoms, in essence, occupying virtually identical space. The green surface depicting the binding site volume and the space-filled representations were generated from the compound **13**-h/rFAAH model and are virtually identical to those generated from the PF-750-h/rFAAH crystal structure. In contrast, when the model of compound **38**-h/rFAAH was minimized, there was a significant shift in the position of the side chain of Met436. As shown in Figure 5, the ethoxy portion of compound **38** extends beyond the green surface generated from the compound **13** model illustrating the increased size of the ligand and the subsequent displacement (i.e., push) of the Met436 side chain. This steric interaction with Met436 could explain the decreased potency of compound **38**.

To assess the selectivity of the benzothiophene piperidine/piperazine urea series, compounds **6b**, **6g** (PF-465), and **13** (PF-946) were profiled at 100  $\mu$ M by competitive activity-based protein profiling (ABPP)<sup>13</sup> in a number of different proteomes derived from mouse and human sources (Fig. 6). Competitive ABPP provides a global view of the proteome-wide selectivity of enzyme inhibitors as described previously.<sup>13b,c</sup> In the case of FAAH inhibitors, we used a reporter-tagged fluorophosphonate (FP) ABPP probe,<sup>13c</sup> which serves as a general activity-based profiling tool for the

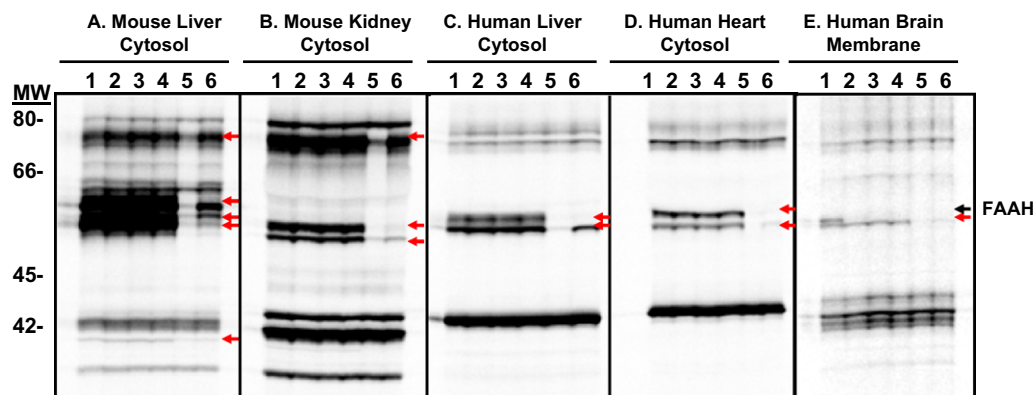


**Figure 6.** Selectivity profiling of FAAH inhibitors. Gel images of proteomes labeled with FP-rhodamine in the absence or presence of FAAH inhibitors (Lane 1, buffer; lane 2, **6b** at 100  $\mu$ M; lane 3, **6g** at 100  $\mu$ M; lane 4, **13** at 100  $\mu$ M; lane 5, URB597 at 100  $\mu$ M; lane 6, URB597 at 10  $\mu$ M). Inhibited bands are shown with arrows. (A) soluble mouse liver proteome, (B) soluble mouse kidney proteome, (C) soluble human liver proteome, (D) soluble human heart proteome, and (E) human brain membrane proteome. Fluorescent gel signals shown in grayscale.

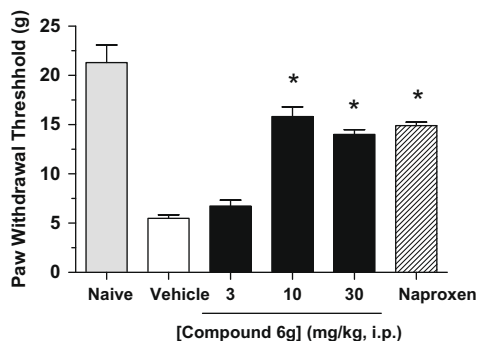


**Figure 7.** Anti-hyperalgesic effects of compound **6g** (3–30 mg/kg, ip) in the CFA model of inflammatory pain. Compound **6g** produces a dose-dependent reduction of mechanical allodynia (hyperalgesic) in rats (black bars). The effect of the non-steroidal anti-inflammatory drug naproxen (10 mg/kg, ip hatched bar) is shown for comparison. Anti-hyperalgesic responses were determined at 4 h following drug treatment and were significantly different between compound **6g**- and vehicle-treated groups ( $p < 0.05$ ).  $n = 8$  rats/group.

serine hydrolase super family.<sup>13d,e</sup> Serine hydrolases that show significant reductions in FP probe labeling intensity in the presence of inhibitor are scored as targets of the compound. The selectivity of compounds **6b**, **6g**, and **13** was compared to that of URB597, which was profiled at 10 and 100  $\mu$ M. Gel images of soluble proteomes of mouse liver, mouse kidney, human liver, and human heart and the membrane proteome of human brain are shown in Figure 6. Consistent with previous reports,<sup>6a,14</sup> multiple off-targets were observed in peripheral tissues for URB597 even at 10  $\mu$ M, particularly amongst FP-labeled proteins migrating between 55 and 65 kDa. It is noteworthy that URB597, which has been shown to be highly selective for serine hydrolases in mouse brain proteomes, inhibits at least one additional hydrolase migrating at 55–60 kDa in the human brain membrane proteome. In contrast, no off-targets were observed for compounds **6b**, **6g**, and **13** even when tested at 100  $\mu$ M (Fig. 6). Under the assay conditions, compounds **6b**, **6g**, **13**, and URB597 completely inhibited FAAH from both mouse and human tissues.

Next we selected compound **6g** (PF-465) to assess its in vivo efficacy in a rat model of inflammatory pain. Subcutaneous injection of complete Freund's adjuvant (CFA) into the plantar surface of the hind paw produced a significant decrease in mechanical paw weight threshold (PWT) at 5 days post injection (Fig. 7). Compound **6g** dosed at 3, 10 and 30 mg/kg (ip) caused a dose-dependent inhibition of mechanical allodynia with a minimum effective dose (MED) of 10 mg/kg. At doses of 10 and 30 mg/kg, compound **6g** inhibited pain responses to an equivalent degree as the nonsteroidal anti-inflammatory drug naproxen (10 mg/kg, ip).

In conclusion, we have described a series of benzothioephene piperazine/piperidine urea FAAH inhibitors that covalently modify the enzyme's active site serine nucleophile. Activity-based protein profiling revealed that these urea inhibitors are highly selective for FAAH relative to other mammalian serine hydrolases. Furthermore, in vivo activity was demonstrated in a rat CFA model of inflammatory pain. Additional SAR development of this class of piperazine/piperidine urea FAAH inhibitors will be reported in due course.

## References and notes

- (a) Cravatt, B. F.; Giang, D. K.; Mayfield, S. P.; Boger, D. L.; Lerner, R. A.; Gilula, N. B. *Nature* **1996**, *384*, 83; (b) Bracey, M. A.; Hanson, M. A.; Masuda, K. R.; Stevens,

- R. C.; Cravatt, B. F. *Science* **2002**, *298*, 1793; (c) Cravatt, B. F.; Lichtman, A. H. *Curr. Opin. Chem. Biol.* **2003**, *7*, 469; (d) McKinney, M. K.; Cravatt, B. F. *Annu. Rev. Biochem.* **2005**, *74*, 411; (e) Ahn, K.; McKinney, M. K.; Cravatt, B. F. *Chem. Rev.* **2008**, *108*, 1687; (f) Cravatt, B. F.; Demarest, K.; Patricelli, M. P.; Bracey, M. H.; Giang, D. K.; Martin, B. R.; Lichtman, A. H. *Proc. Natl. Acad. Sci. U.S.A.* **2001**, *98*, 9371; (g) Kathuria, S.; Gaetani, S.; Fegley, D.; Valino, F.; Duranti, A.; Tontini, A.; Mor, M.; Tarzia, G.; La Rana, G.; Calignano, A.; Giustino, A.; Tattoli, M.; Palmery, M.; Cuomo, V.; Piomelli, D. *Nat. Med.* **2003**, *9*, 76.
- (a) Lambert, D. M.; Fowler, C. J. *J. Med. Chem.* **2005**, *48*, 5059; (b) Pacher, P.; Batkai, S.; Kunos, G. *Pharmacol. Rev.* **2006**, *58*, 389; (c) Di Marzo, V. *Nat. Rev. Drug Disc.* **2008**, *7*, 438; (d) Seierstad, M.; Breitenbucher, J. G. *J. Med. Chem.* **2008**, *51*, 7327.
- (a) Boger, D. L.; Sato, H.; Lerner, A. E.; Hedrick, M. P.; Fecik, R. A.; Miyauchi, H.; Wilkie, G. D.; Austin, B. J.; Patricelli, M. P.; Cravatt, B. F. *Proc. Natl. Acad. Sci. U.S.A.* **2000**, *97*, 5044; (b) Boger, D. L.; Miyauchi, H.; Du, W.; Hardouin, C.; Fecik, R. A.; Cheng, H.; Hwang, I.; Hedrick, M. P.; Leung, D.; Acevedo, O.; Guimaraes, C. R. W.; Jorgensen, W. L.; Cravatt, B. F. *J. Med. Chem.* **2005**, *48*, 1849; (c) Garfunkle, J.; Ezzi, C.; Rayl, T. J.; Hochstatter, D. G.; Hwang, I.; Boger, D. L. *J. Med. Chem.* **2008**, *51*, 4392.
- (a) Tarzia, G.; Duranti, A.; Tontini, A.; Piersanti, G.; Mor, M.; Rivara, S.; Plazzi, P. V.; Park, C.; Kathuria, S.; Piomelli, D. *J. Med. Chem.* **2003**, *46*, 2352; (b) Mor, M.; Rivara, S.; Lodola, A.; Plazzi, P. V.; Tarzia, G.; Duranti, A.; Tontini, A.; Piersanti, G.; Kathuria, S.; Piomelli, D. *J. Med. Chem.* **2004**, *47*, 4998; (c) Tarzia, G.; Duranti, A.; Gatti, G.; Piersanti, G.; Tontini, A.; Rivara, S.; Lodola, A.; Plazzi, P. V.; Mor, M.; Kathuria, S.; Piomelli, D. *Chem. Med. Chem.* **2006**, *1*, 2352.
- Abouab-Dellah, A.; Burnier, P.; Hoornaert, C.; Jeunesse, J.; Puech, F. Patent WO 2004/099176, 2004; US 2006/0089344, 2006.
- (a) Ahn, K.; Johnson, D. S.; Fitzgerald, L. R.; Liimatta, M.; Arendse, A.; Stevenson, T.; Lund, E. T.; Nugent, R. A.; Nomanbhoy, T. K.; Alexander, J. P.; Cravatt, B. F. *Biochemistry* **2007**, *46*, 13019; (b) Mileni, M.; Johnson, D. S.; Wang, Z.; Everdeen, D.; Liimatta, M.; Pabst, B.; Bhattacharya, K.; Nugent, R. A.; Kamtekar, S.; Cravatt, B. F.; Ahn, K.; Stevens, R. C. *Proc. Natl. Acad. Sci. U.S.A.* **2008**, *105*, 12820; (c) Apodaca, R.; Breitenbucher, J. G.; Pattabiraman, K.; Seierstad, M.; Xiao, W. Patent WO 2006/074025, 2006.
- (a) Matsumoto, T.; Kori, M.; Miyazaki, J.; Kiyota, Y. Patent WO 2006/054652, 2006; EP 1813606, 2007; (b) Keith, J. M.; Apodaca, R.; Xiao, W.; Seierstad, M.; Pattabiraman, K.; Wu, J.; Webb, M.; Karbarz, M. J.; Brown, S.; Wilson, S.; Scott, B.; Tham, C.-S.; Luo, L.; Palmer, J.; Wennerholm, M.; Chaplan, S.; Breitenbucher, J. G. *Bioorg. Med. Chem. Lett.* **2008**, *18*, 4838; (c) Karbarz, M. J.; Luo, L.; Chang, L.; Tham, C.-S.; Palmer, J. A.; Wilson, S. J.; Wennerholm, M. L.; Brown, S. M.; Scott, B. P.; Apodaca, R. L.; Keith, J. M.; Wu, J.; Breitenbucher, J. G.; Chaplan, S. R.; Webb, M. *Anesthesia Analgesia* **2009**, *108*, 316.
- (a) Thavonekham, B. *Synthesis* **1997**, 1189; (b) Swanson, D. M.; Dubin, A. E.; Shah, C.; Nasser, N.; Chang, L.; Dax, S. L.; Jetter, M.; Breitenbucher, J. G.; Liu, C.; Mazur, C.; Lord, B.; Gonzales, L.; Hoey, K.; Rizzolio, M.; Bogenstaetter, M.; Codd, E. E.; Lee, D. H.; Zhang, S.-P.; Chaplan, S. R.; Carruthers, N. I. *J. Med. Chem.* **2005**, *48*, 1857.
- Matsunaga, N.; Kaku, T.; Itoh, F.; Tanaka, T.; Hara, T.; Miki, H.; Iwasaki, M.; Aono, T.; Yamaoka, M.; Kusaka, M.; Tasaka, A. *Bioorg. Med. Chem.* **2004**, *12*, 2251.
- Ahn, K. Patent WO 2006/085196, 2006.
- Copeland, R. A. *Enzymes: A Practical Introduction to Structure, Mechanism, and Data Analysis*, 2nd ed.; Wiley-VCH: New York, 2000. pp 318–349.
- All the hydrogens were added to the protein and each compound was covalently attached to the sidechain oxygen of Ser241. The protein/ligand structures were then minimized using the Sybyl forcefield with the backbone atoms held constant; charges were not used. These minimized structures were then compared to the PF-750-h/rFAAH crystal structure.
- (a) Cravatt, B. F.; Wright, A. T.; Kozarich, J. W. *Annu. Rev. Biochem.* **2008**, *77*, 383; (b) Kidd, D.; Liu, Y.; Cravatt, B. F. *Biochemistry* **2001**, *40*, 4005; (c) Leung, D.; Hardouin, C.; Boger, D. L.; Cravatt, B. F. *Nat. Biotechnol.* **2003**, *21*, 687; (d) Patricelli, M. P.; Giang, D. K.; Stamp, L. M.; Burbaum, J. J. *Proteomics* **2001**, *1*, 1067; (e) Liu, Y.; Patricelli, M. P.; Cravatt, B. F. *Proc. Natl. Acad. Sci. U.S.A.* **1999**, *96*, 14694.
- (a) Alexander, J. P.; Cravatt, B. F. *Chem. Biol.* **2005**, *12*, 1179; (b) Zhang, D.; Saraf, A.; Kolasa, T.; Bhatia, P.; Zheng, G. Z.; Patel, M.; Lannoye, G. S.; Richardson, P.; Stewart, A.; Rogers, J. C.; Brioni, J. D.; Surowy, C. S. *Neuropharmacol.* **2007**, *52*, 1095.
- The hFAAH (amino acids 32–579) and rFAAH (amino acids 30–579) constructs were generated as the N-terminal transmembrane-deleted truncated forms with N-terminal His<sub>6</sub> tags, and were expressed in *E. coli* and purified as previously described.<sup>6b</sup> Both hFAAH and rFAAH enzymes used in the present study had purity greater than 95% based on SDS-PAGE visualized by Coomassie blue staining. The GDH-coupled FAAH assay was performed for determination of potencies ( $k_{\text{inact}}/K_i$  values) of inhibitors in 384-well microplates with a final volume of 50  $\mu$ L. The details on the assay and derivations of the overall potency,  $k_{\text{inact}}/K_i$  value, have been described previously.<sup>6b</sup> In the 384-well format assay, the  $k_{\text{inact}}/K_i$  values were generally calculated from the slope,  $k_{\text{inact}}/[K_i(1 + [S]/K_m)]$ , which is obtained from the  $k_{\text{obs}}$  versus  $[I]$  linear lines. The  $k_{\text{inact}}/K_i$  values are averages of at least two independent experiments.